

Supporting Information

Hanson et al. 10.1073/pnas.1306097110

SI Experimental Procedures

Cells and Parasites. The Huh7 human hepatoma cell line was cultured in RPMI medium supplemented with 10% FCS, 1% non-essential amino acids, 1% penicillin/streptomycin, 1% glutamine, and 1% Hepes, pH 7 (all Gibco/Invitrogen). The HepG2 human hepatoma cell line was cultured in DMEM supplemented with 10% FCS, 1% penicillin/streptomycin, and 1% glutamine. Both were maintained at 37 °C with 5% CO₂. Fungizone was added at 1:1,000 when cells were infected. Mouse primary hepatocytes were isolated as described previously (1).

Plasmodium berghei parasites expressing soluble GFP under the control of the exoerythrocytic form 1a (EEF1a) promoter (parasite line 259cl2) (2) were freshly isolated from infected *Anopheles stephensi* mosquitos for each experiment.

Mice. Male C57BL/6 mice (Charles River), 6–8 wk of age, were used. All mice were housed and manipulated in the animal facility of the Instituto de Medicina Molecular in Lisbon. All in vivo protocols were approved by the internal animal care committee of the Instituto de Medicina Molecular and were performed according to national and European regulations.

Chemicals. All chemicals used were from Sigma Aldrich, except Torin1 (kindly provided by D. Sabatini, Whitehead Institute for Biomedical Research, Cambridge, MA) and Torin2 (synthesized according to a modification of the protocol described in ref. (3)).

Flow Cytometry Analysis of Liver Stage Infection. Flow cytometry was performed largely as described (4). Briefly, each well of infected cells was trypsinized, washed in PBS, and resuspended in 250 µL of 10% FCS. Cells were analyzed on BD FACS Calibur or LSR Fortessa cytometers. All events in each sample were acquired for analysis. Viable vs. nonviable cells were gated on the basis of forward scatter (FSC) vs. side scatter (SSC), and GFP+ infected cells were identified by plotting green fluorescence FL-1 vs. red fluorescence FL-3 and gating the GFP+ populations. Noninfected cells were used to ensure that the GFP+ gate did not contain any false-positive events. Data analysis was carried out in FlowJo.

Immunofluorescence and Live Imaging. The following primary antisera and antibody were used in the study: rabbit anti-*P. berghei* EXP1 (1:250) (5), kindly provided by V. Heussler (University of Bern, Bern, Switzerland); rabbit anti-*Plasmodium yoelii* Up-Regulated in Sporozoites 4 (UIS4) (1:500) (6), kindly provided by S. Kappe (Seattle Biomedical Research Institute, Seattle, WA); goat anti-*P. berghei* UIS4 (1:1,000) (7), kindly provided by M. Seabra (Faculdade de Ciências Médicas, Universidade Nova de Lisboa, Lisbon, Portugal); rabbit anti-*P. berghei* thrombospondin-related anonymous protein (TRAP) (1:300) (8); and mouse anti-*P. berghei* heat shock protein 70 HSP70 (2E6, 1:1,000) (9). Various AlexaFluor-conjugated secondary antibodies were used (1:500, Molecular Probes/Invitrogen), as well as tetramethylrhodamine ethyl ester (TMRE) (Molecular Probes/Invitrogen) and Hoechst 33258 (Molecular Probes/Invitrogen). All Images were acquired on Zeiss confocal microscopes (510 Meta and 710).

For immunofluorescence analysis (IFA) when anti-EXP1 was not used, cells were fixed in 4% paraformaldehyde for 15 min at room temperature (RT), washed three times in PBS, and then permeabilized in 0.01% TritonX-100 for 10 min. Cells were subsequently blocked in 2% bovine serum albumin (BSA) and 0.01% TritonX-100 for 30 min and stained for 2 h at RT with 1° antibodies

diluted in the blocking solution. After three PBS washes, the cells were incubated with 2° antibodies, along with DAPI, for 30 min, washed three times again with PBS, and mounted in Fluoromount (Southern Biotech).

For IFA involving anti-EXP1, the procedure was the same, except TritonX-100 was not used in any solutions; cells were methanol-permeabilized at –20 °C for 10 min, and 1° antibody incubation was carried out overnight at 4 °C.

Image Quantification. All images were processed and quantified in ImageJ. Multichannel lsm confocal images were split into single channels, the UIS4 and PbHSP70 channels were independently thresholded, and regions of interest (ROIs) were created from all UIS4+ pixels and all PbHSP70+ pixels. The two channel-specific ROIs were joined to create an ROI of all UIS4 and/or PbHSP70+ pixels, and the percentage of double-positive pixels (UIS4 inside the parasite soma) and UIS4 single-positive pixels (UIS4 outside of the parasite soma) was determined. The quantification protocol was recorded in an ImageJ macro, which was used on all images with uniform channel-specific thresholding across the entire dataset.

Blood Stage Assays. *Plasmodium falciparum* 3D7 was cultured in RPMI-based complete malaria culture medium (CMCM) according to the recommendations of the Malaria Research and Reference Reagent Resource Center (MR4) and maintained at 37 °C in an atmosphere of 5% CO₂. Continuous cultures of *P. falciparum* with a parasitemia of >2% and with a minimum of 50% rings were synchronized by adding 5% sorbitol for 10 min at room temperature, as described (10). Synchronized ring stage cultures (at least 90% ring forms) at 2.5% hematocrit and ~1% parasitemia were incubated for 72 h at 37 °C in a 5% CO₂ atmosphere in a 96-well plate with Torin1 and -2 or with CMCM used in the drug-free and uninfected controls. A 5-µL aliquot from each assay well was stained with the DNA-specific dye SYBR green I (Invitrogen) one time. After 20 min of incubation, the sample was immediately analyzed by flow cytometry using a 535/45-nm bandpass filter in front of the detector on a Partec CyFlow Blue benchtop cytometer; ~100,000 events were acquired for each sample. Measurements were done at 0, 12, 24, 36, 48, and 72 h of incubation. All conditions were tested in triplicate. Flow cytometry data were analyzed using FlowJo software (version 9.0.2, TreeStar Inc.). SYBR green I-positive events were established based on a stained uninfected control and had to be adjusted at each time point, always using the uninfected SYBR green-stained sample of the correspondent time point to establish the gate.

Drug Susceptibility Testing Against *P. falciparum* Asexual and Sexual Stages. The efficiency of the compound on asexual and sexual forms of *P. falciparum* (transgenic line 164/GFP) has been tested in the drug susceptibility assay as described previously (11). In summary, tightly synchronized ring stage parasites were plated at 4% hematocrit in 96-well plates alongside uninfected red blood cells as a negative control. A drop in hematocrit was used to induce sexual commitment 24 h after seeding the parasites. Serial dilutions of the compound were added at this point or 24 h postinduction, after reinvasion of the parasites. Positive control wells were handled accordingly without any drug addition. On the day of analysis, cells were stained for 30 min with 4 µM Hoechst 33342 (Invitrogen) and analyzed with flow cytometry. The data were managed with Quanta software and analyzed using GraphPad Prism.

Stepwise Intermittent Selection of Blood Stage *P. falciparum*. Cultures of 25 mL of 4% synchronous ring stage Dd2 parasites at 4% hematocrit, roughly 10^9 parasites, were subject to an in vitro stepwise intermittent selection protocol. The cultures were exposed first to $10\times$ EC₅₀ for 24–192 h of constant selection or for 48 h and pulsed three times, separated by 48 h off selection to find optimal selection conditions: killing the majority of parasites while leading to recrudescence of resistant parasites. Cultures were maintained according to standard culturing methods. In addition, cultures were split 1:4 every 7 d to replenish red blood cell populations and smeared every 4 d to monitor for recrudescence. All selections without recrudescence parasites were monitored for a minimum of 60 d after removal of drug pressure.

Once parasites had recrudescence, additional rounds of selection at the same dosage and length of drug pressure were conducted and maintained as described above. Response to drug selection was evaluated by change in dose–response in a SYBR green-based growth assay and by time to recrudescence.

Statistical Analysis. Data are presented as mean \pm SD unless otherwise noted. Dose–response curves were generated and EC₅₀'s were determined in GraphPad Prism, using four-variable log [inhibitor] vs. normalized response nonlinear curve fitting. Survival curves (log-rank test) and in vivo parasitaemia curves (two-way repeated measurement ANOVA with Bonferroni posttest) were compared using GraphPad Prism. All other data were analyzed in Excel with unpaired two-tailed *t* tests.

Transmission Electron Microscopy. For ultrastructural analysis, infected cells were fixed in 2% paraformaldehyde/2.5% glutaraldehyde in phosphate buffer for 1 h at RT. Samples were washed in phosphate buffer and postfixed in 1% osmium tetroxide (Polysciences) for 1 h. Samples were then rinsed extensively in dH₂O before en bloc staining with 1% aqueous uranyl acetate (Ted Pella) for 1 h. Following several rinses in dH₂O, samples were dehydrated in a graded series of ethanol and embedded in Eponate 12 resin (Ted Pella). Sections of 90 nm were cut with a Leica Ultracut UCT ultramicrotome (Leica Microsystems), stained with uranyl acetate and lead citrate, and viewed on a JEOL 1200 EX transmission electron microscope (JEOL).

siRNA Knockdown. HepG2 cells were trypsinized, resuspended in antibiotic-free medium, and counted. siRNA oligonucleotide ON-TARGETplus SMARTpools (Dharmacon) targeting human *raptor* (L-004107, human RAPTOR, NM_020761), *mTOR* (L-003008, human FRAP1, NM_004958), or a control nontargeting pool (D-001810) were mixed with OptiMEM (Gibco) and Lipofectamine RNAiMAX (Invitrogen) according to the manu-

facturer's instructions for a final concentration of 30 nM siRNA per well of a 24-well plate. A total of 35,000 HepG2 cells in antibiotic-free DMEM were added for a final volume of 500 μ L per well and incubated for a minimum of 4 h before the medium was replaced with complete DMEM. Knockdown cells were infected with 20,000 *P. berghei*-GFP sporozoites per well 48 h later, and after a further 48 h cells were processed for flow cytometry to quantify infection.

Gene-Specific Expression and Infection Quantitation by Quantitative RT-PCR. For HepG2 cell experiments, RNA was extracted using High Pure RNA Isolation Kits (Roche). Ten micrograms of RNA was reverse-transcribed with random hexamers using the Transcriptor First Strand cDNA Synthesis kit (Roche). Gene expression analysis was performed using kits from Applied Biosystems on an ABI 7500 Fast.

Relative amounts of remaining mRNA of siRNA targets were normalized to a housekeeping gene, hypoxanthine guanine phosphoribosyltransferase (HPRT), and mRNA levels of siRNA-transduced samples were compared with those of the nontargeting control-treated cells.

The following intron-spanning primers were used to quantify gene expression after knockdown: Raptor—5' CACCGCTGAGAGCATTGGACTTG 3' and 5' TCAGAGCCACCACAGCTCGCTG 3'; mTOR—5' AGGCCTGGGGGAATGGGG T 3' and 5' TGCAGTGCCAGCACAGCTCT 3'; and HPRT (primer set designed to specifically amplify both human and mouse *hppt*)—5' TTTGCTGACCTGCTGGATTAC 3' and 5' CAAGACATTCTTTCCAGTTAAAGTTG 3'. Transcript knockdown was assessed by comparing individual gene expression levels in the specifically targeted vs. control cells. Knockdown of 65–85% was achieved in all experiments.

To quantify *P. berghei* liver load, whole livers were homogenized in 3 mL of denaturing solution (4 M guanidine thiocyanate; 25 mM sodium citrate, pH 7, 0.5% *N*-lauroylsarcosine, and 0.7% β -mercaptoethanol in diethyl pyrocarbonate-treated water). RNA was extracted using the RNeasy Mini kit (Qiagen). cDNA generation and quantitative PCR was performed as above, and *P. berghei* 18S rRNA abundance was normalized to expression of HPRT, using the HPRT primer pair indicated above and 5' AAGCATTAAA-TAAAGCGAATACATCCTTAC 3' and 5' GGAGATTGGTTT TGACGTTTATGTG 3' for *P. berghei* 18S.

Gene expression and infection values were calculated based on the Delta-Delta-Ct (DDCt) method, using the control replicate value closest to the mean of control group as calibrator to which all other samples were compared. Relative quantities (RQ) were determined using the equation $RQ = 2^{-\Delta\Delta Ct}$.

- Gonçalves LA, Vigário AM, Penha-Gonçalves C (2007) Improved isolation of murine hepatocytes for in vitro malaria liver stage studies. *Malar J* 6:169.
- Franke-Fayard B, et al. (2004) A *Plasmodium berghei* reference line that constitutively expresses GFP at a high level throughout the complete life cycle. *Mol Biochem Parasitol* 137(1):23–33.
- Liu Q, et al. (2010) Discovery of 1-(4-(4-propionylpiperazin-1-yl)-3-(trifluoromethyl)phenyl)-9-(quinolin-3-yl)benzo[h][1,6]naphthyridin-2(1H)-one as a highly potent, selective mammalian target of rapamycin (mTOR) inhibitor for the treatment of cancer. *J Med Chem* 53(19):7146–7155.
- Prudêncio M, Rodrigues CD, Ataíde R, Mota MM (2008) Dissecting in vitro host cell infection by *Plasmodium* sporozoites using flow cytometry. *Cell Microbiol* 10(1):218–224.
- van de Sand C, et al. (2005) The liver stage of *Plasmodium berghei* inhibits host cell apoptosis. *Mol Microbiol* 58(3):731–742.
- Kaiser K, et al. (2004) A member of a conserved *Plasmodium* protein family with membrane-attack complex/perforin (MACPF)-like domains localizes to the micronemes of sporozoites. *Mol Biochem Parasitol* 133(1):15–26.
- Lopes da Silva M, et al. (2012) The host endocytic pathway is essential for *Plasmodium berghei* late liver stage development. *Traffic* 13(10):1351–1363.
- Gantt S, et al. (2000) Antibodies against thrombospondin-related anonymous protein do not inhibit *Plasmodium* sporozoite infectivity in vivo. *Infect Immun* 68(6):3667–3673.
- Tsuji M, Mattei D, Nussenzeig RS, Eichinger D, Zavala F (1994) Demonstration of heat-shock protein 70 in the sporozoite stage of malaria parasites. *Parasitol Res* 80(1):16–21.
- Lambros C, Vanderberg JP (1979) Synchronization of *Plasmodium falciparum* erythrocytic stages in culture. *J Parasitol* 65(3):418–420.
- Buchholz K, et al. (2011) A high-throughput screen targeting malaria transmission stages opens new avenues for drug development. *J Infect Dis* 203(10):1445–1453.

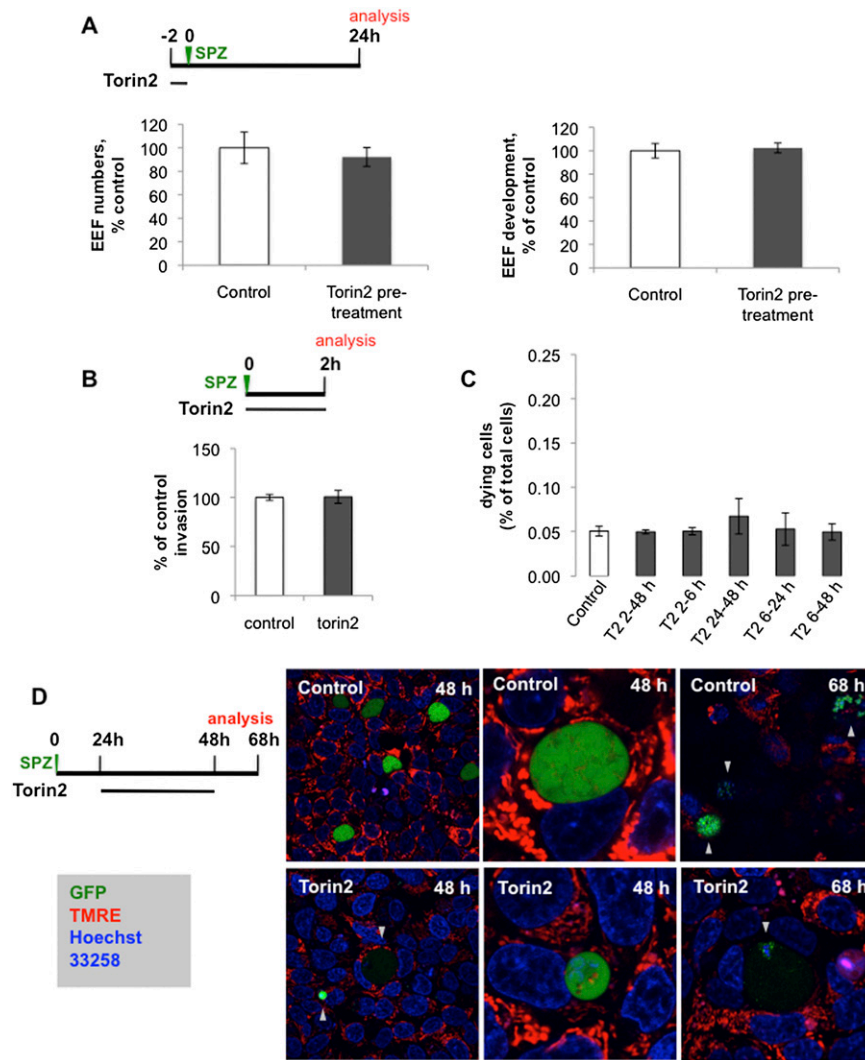


Fig. S1. Torin2 treatment does not alter sporozite invasion or proportion of dying HepG2 cells, but prevents merozoite formation. (A) Effects of Torin2 pretreatment on *P. berghei* liver stage development in HepG2 cells. Schematic illustrates experimental setup. Infected HepG2 cells were analyzed by flow cytometry 24 h after sporozoite addition, as in Fig. 1. Data represent mean \pm SD of three independent experiments. (B) Effects of Torin2 treatment on *P. berghei* sporozoite invasion in HepG2 cells. Schematic illustrates experimental setup. Infected HepG2 cells were analyzed by flow cytometry 2 h after sporozoite addition, as in Fig. 1. Data represent mean \pm SD of three independent experiments. (C) Effects of Torin2 treatment on HepG2 cell viability. Identical data set as in Fig. 4B. Data represent mean \pm SD of quadruplicates from one representative experiment with all conditions processed in parallel. (D) Effects of Torin2 treatment from 24 to 50 h on subsequent *P. berghei* liver stage development in HepG2 cells. Schematic illustrates experimental setup. Live imaging of TMRE (red, mitochondria with intact membrane potential), *P. berghei*-expressed GFP (green), and Hoechst 33258 (blue, DNA).

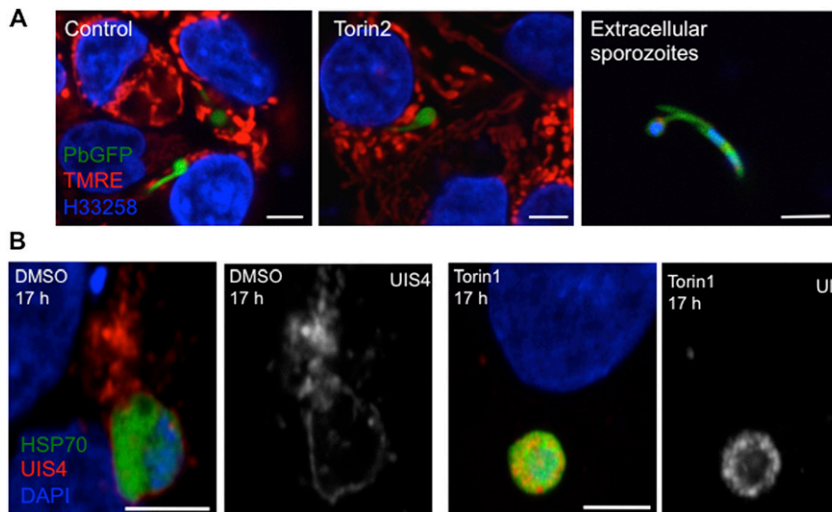


Fig. S2. Torin2 treatment does not disrupt the liver stage trophozoite parasitophorous vacuole membrane (PVM), but Torin2 relocates UIS4. (A) Effects of Torin2 treatment from 2 to 8 h on *P. berghei* susceptibility to labeling by Hoechst 33258. Live imaging of control and Torin2-treated cells, as well as extracellular sporozoites; representative confocal images [positive control for Hoechst 33258 labeling TMRE (red, mitochondria with intact membrane potential), *P. berghei*-expressed GFP (green), and Hoechst 33258 (blue, DNA)]. (B) Effects of Torin1 treatment from 2 to 17 h on *P. berghei* UIS4 localization. Representative confocal images of HSP70 (green), UIS4 (red), and DAPI (blue).

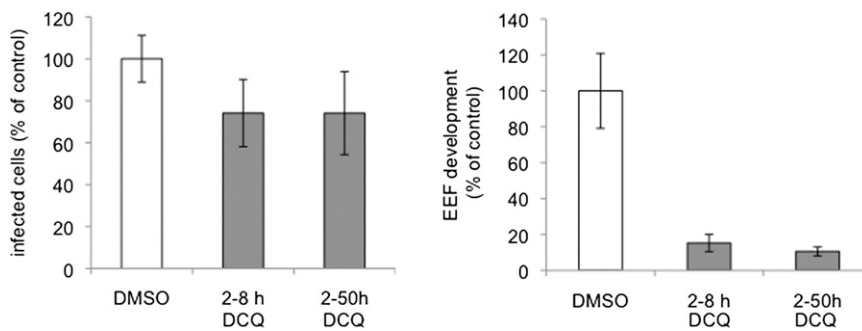


Fig. S3. Decoquinatone treatment from 2 to 8 h is phenotypically equivalent to 2–50 h treatment. Effects of 10x EC₅₀ decoquinatone on *P. berghei* liver stage infection load (Left) and development (Right) in HepG2 cells. Infected HepG2 cells were analyzed by flow cytometry 24 h after sporozoite addition, as in Fig. 1. Data represent mean ± SD of three independent experiments.

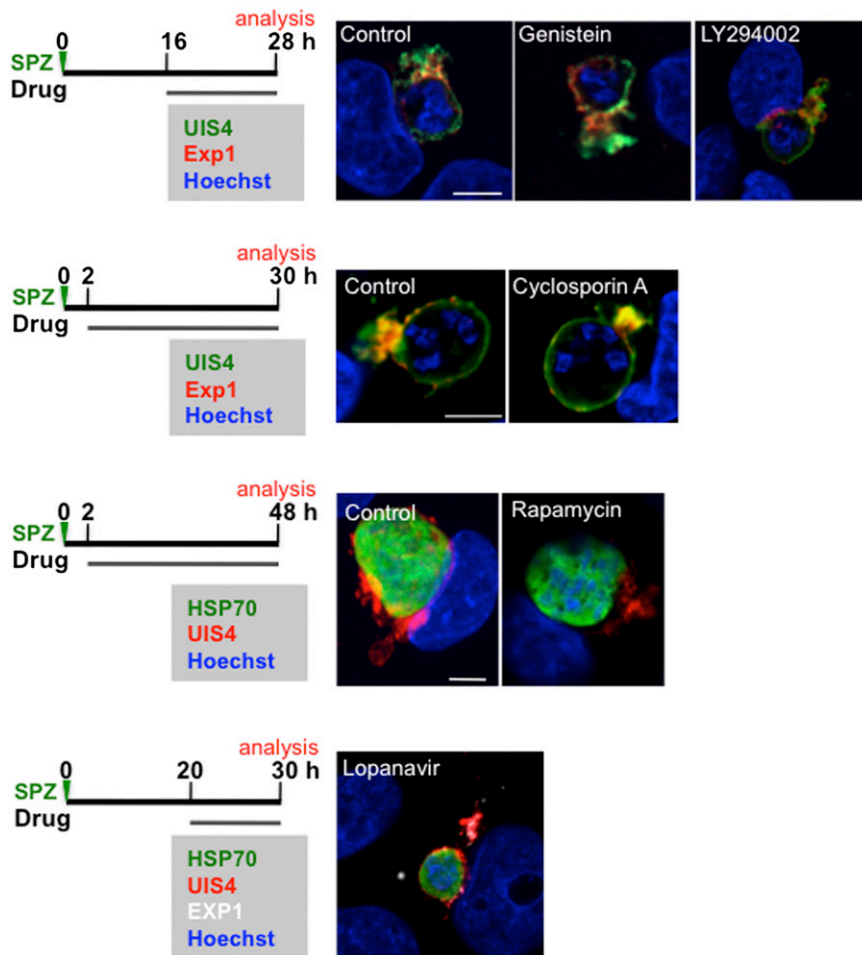


Fig. 54. Localization of PVM resident proteins is not affected by liver stage inhibitors, LY294002, or rapamycin. Effects of liver stage inhibitors or PI3K/mTOR inhibitors on PVM-resident protein localization. Schematic illustrates experimental setup for each. Representative confocal images shown for 25 μ M genistein, 25 μ M LY294002, 700 nM cyclosporin A, and 250 nM rapamycin with DMSO (vehicle) as a control.

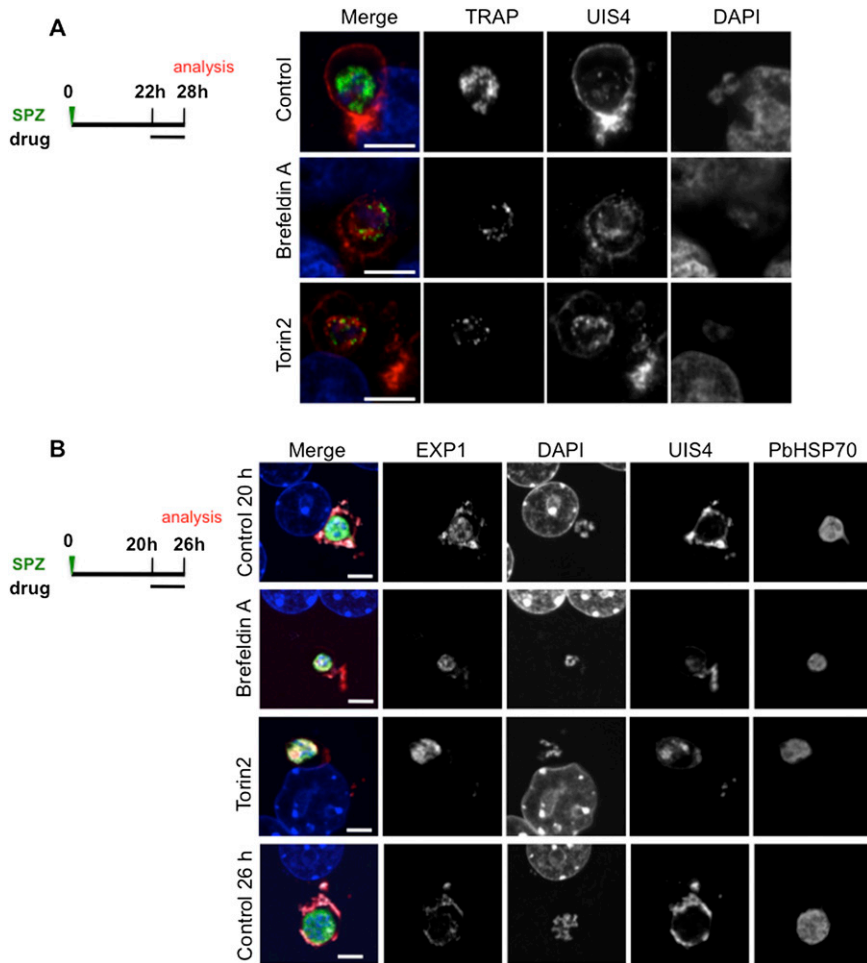
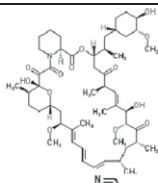
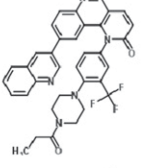
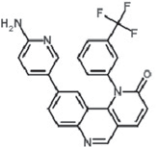
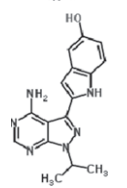


Fig. 55. EXP1 and UIS4 trafficking are BFA- and Torin2-sensitive in young liver stage schizonts, but UIS4 is not relocated into TRAP-positive structures. (A) Effects of Torin2 and BFA on UIS4 and TRAP distribution in young liver stage schizonts in HepG2 cells. Schematic illustrates experimental setup. Representative confocal images of control Torin2- and BFA-treated EEFs with UIS4 (red), TRAP (green), and DAPI (blue) labeling. (B) Effects of Torin2 and BFA on UIS4 and EXP1 distribution in young liver stage schizonts in mouse 1^o hepatocytes ex vivo. Schematic illustrates experimental setup. Representative confocal images of control Torin2- and BFA-treated EEFs with UIS4 (red), EXP1 (white), HSP70 (green), and DAPI (blue) labeling.

Table S1. mTOR inhibitors tested for antiplasmodial activity

Compound	Structure	MoA for mTOR inhibition	<i>P. berghei</i> liver stage inhibition	<i>P. falciparum</i> blood stage inhibition
Rapamycin		Allosteric inhibition through FKBP12 binding	No (at concentrations up to 250 nM)	ND
Torin1		ATP-competitive inhibitor	Yes (EC_{50} = 106 nM)	Yes (3D7)
Torin2		ATP-competitive inhibitor	Yes (EC_{50} = 1.1 nM)	Yes (3D7 asexual, EC_{50} = 1.4 nM; 3D7 sexual, EC_{50} = 6.6 nM; Dd2 asexual, EC_{50} = 0.7 nM)
PP242		ATP-competitive inhibitor	No (at concentrations up to 2.5 μ M)	No (3D7 at concentrations up to 2.5 μ M)

MoA, mechanism of action.